IEEE Photonics Journal
An IEEE Photonics Society Publication

Open Access

Theoretically Enhance the Vertical Light Extraction Efficiency of the AlGaN-Based Nanowire Photonic Crystal Ultraviolet Light-Emitting Diodes by Selecting the Band Gap

Volume 13, Number 3, June 2021

Zichen Zhang
Fangliang Gao
Guoqiang Li

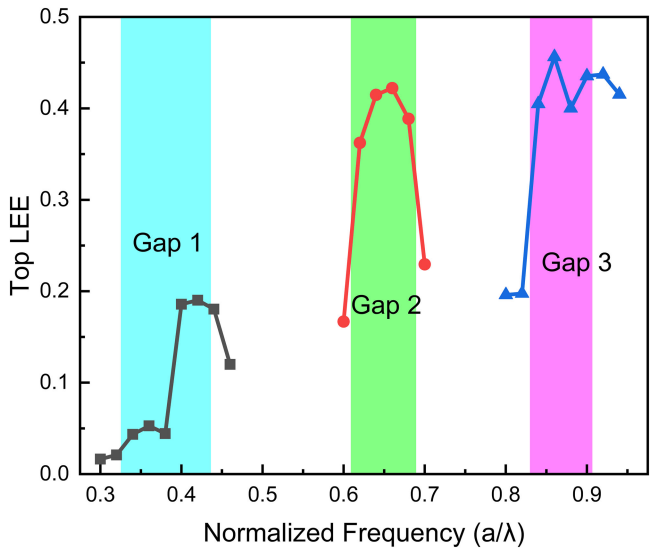

DOI: 10.1109/JPHOT.2021.3084678

IEEE photonics SOCIETY

IEEE

Theoretically Enhance the Vertical Light Extraction Efficiency of the AlGaN-Based Nanowire Photonic Crystal Ultraviolet Light-Emitting Diodes by Selecting the Band Gap

Zichen Zhang,[1] **Fangliang Gao**,[2,3] **and Guoqiang Li**[1,3]

[1]State Key Laboratory of Luminescent Materials and Devices, South China University of Technology, Guangzhou 510640, China
[2]Guangdong Engineering Research Center of Optoelectronic Functional Materials and Devices, Institute of Semiconductors, South China Normal University, Guangzhou 510631, China
[3]Guangdong Choicore Optoelectronics Company, Ltd, Heyuan 517003, China

DOI:10.1109/JPHOT.2021.3084678

Manuscript received March 14, 2021; revised May 21, 2021; accepted May 25, 2021. Date of publication May 28, 2021; date of current version June 11, 2021. This work was supported in part by National Key Research and Development Project under Grants 2018YFB1801900 and 2018YFB1801902, in part by the National Natural Science Foundation of China under Grants 51702102 and 52002135, in part by the Key-Area Research and Development Program of Guangdong Province under Grants 2019B010145001, 2019B010128002, 2019B010127001, 2019B010129001, and 2020B010170001, in part by the Guangzhou Basic and Applied Basic Research Project under Grant 202002030005, in part by the Key Innovation Project in Industry Chain of Shaanxi Province under Grant 2018ZDCXL-GY-01-02-01, and in part by the Research Collaborative Innovation of Guangzhou City under Grant 201604046027. Corresponding author: Guoqiang Li (e-mail: msgli@scut.edu.cn).

Abstract: Nanowire photonic crystal (PhC) structure is one of promising approaches to enhance vertical light extraction efficiency (LEE) of ultraviolet light emitting diodes (UV LEDs). There are lots of investigations to study the structure of nanowire UV LEDs by using the finite-difference time-domain (FDTD) method. The optimal LEE are obtained by using some optimization algorithms. However, it needs a broad window, not the best values of geometrical parameters of nanowires in practical fabrication. In this paper, the vertical LEE of UV LEDs are theoretically enhanced by selecting the band gaps of AlGaN-based nanowire PhC structure. It illustrates that all the gaps can inhibit the horizontal propagation of light. However, the inhibiting ability of Gap 1 are weaker than them of Gap 2 and Gap 3. The reason is that the radii of nanowires in Gap 1 are too small to support enough guided modes. As a comparison, both Gap 2 and Gap 3 can efficiently inhibit the radiated mode propagation, and finally enhance the vertical LEE. In addition, the variations of height, number, and refractive index of nanowires on vertical LEE and optical band gaps are discussed. This work has benefits for the practical production of nanowire PhC UV LEDs.

Index Terms: Nanowire, photonic crystal, light extraction efficiency, ultraviolet light-emitting diodes.

1. Introduction

Ultraviolet light emitting diodes (UV LEDs), especially deep UV LEDs, have been attracted a lot of attention due to its wide applications. However, the light extraction efficiency (LEE) of UV LEDs is

still limited by several factors, such as poor material quality, transverse magnetic (TM) polarization, low Mg-dopant incorporation, and so on. Among them, the unique TM polarization is one of main issues to prevent the light extraction from the top of UV LEDs. Some approaches such as surface plasmon [1], metallic grating [2], microstructure [3] and nanowire structure [4] have been developed to enhance the LEE of UV LEDs. Recently, AlGaN-based nanowire as a promising approach to enhance the LEE of UV LEDs has been developed. AlGaN nanowire has been reported that it can be grown with nearly free defects and have an excellent p-type doping property [5]. The nanowires with periodic spatial distribution can be used to fabricate a photonic crystal (PhC) structure [6]. By using an optical band gap of PhC, the TM emission propagating in the horizontal direction can be inhibited and coupled with guided modes inside the nanowire [7], [8]. The finite-difference time-domain (FDTD) method are used by many achievements. For example, Mehrdad Djavid *et al.* achieved a lateral LEE of 70% by optimizing the nanowire size, nanowire spacing, and p-GaN thickness [4]. M. Djavid *et al.* calculated the impact of material absorption on the LEE of nanowire UV LEDs [9]. Ronghui Lin *et al.* found the LEE of nanowire UV LEDs could be increased to 24.3% with a tapering angle of nanowire due to the breaking of symmetry in the vertical direction [10]. Xianhe Liu *et al.* theoretically designed a nanowire PhC UV LEDs with optimal nanowire radius and spacing to achieve a high top LEE over 90% [7]. Pengwei Du *et al.* designed two kinds of nanowire UV LEDs to modify the LEE: a flip-chip nanowire UV LEDs with top PhC and a nanowire UV LEDs with transparent graphene electrode [6], [8]. Using some optimization algorithm, like particle swarm optimization, are convenient to achieve a higher LEE [4]. However, in real-world fabrication, it needs broad windows, not some best values of geometrical parameters of nanowires to fabricate PhC structure. Thus, it is necessary to discuss the efficient range of geometrical parameters. In this paper, it is found that the devices which geometrical parameters in both Gap 2 and Gap 3 of PhC have a relatively higher top LEE than them in Gap 1. It is attributed to an increase of guided modes inside the nanowires in Gap 2 and Gap 3. Additional studies in this paper are about the impacts of heights and numbers of nanowires on top LEE. Since an AlGaN nanowire can be considered as a light cavity, a growth of height of nanowire can causes mode resonance inside the nanowire and make the top LEE changed periodically. On the other hand, an increase of the number of nanowires can enhance the top LEE too. The reason is that, on the whole, the extra additional lights from the increasing nanowires are more than the escaped lights from the nanowires at the edge of devices. Thus, these studies have a great benefit to fabricate AlGaN nanowire PhC UV LEDs.

2. Simulation Setup

The simulations in this paper are calculated by a free and open-source software package MEEP which is based on the FDTD method and is developed by MIT [11]. The FDTD method employs finite differences as approximations to both the spatial and temporal derivatives that appear in Maxwell's equations, as shown in (1) [12], [13]. Here, ε is the permittivity, and μ is the permeability of the material. σ^e is the electric conductivity. E_x, E_y, and E_z are the scalar electric field in a Cartesian coordinate system. H_x, H_y, and H_z the scalar magnetic field in a Cartesian coordinate system.

$$\begin{cases} \frac{\partial E_x}{\partial t} = \frac{1}{\varepsilon_x}\left(\frac{\partial H_z}{\partial y} - \frac{\partial H_y}{\partial z} - \sigma_x^e E_x\right), & \frac{\partial H_x}{\partial t} = -\frac{1}{\mu_x}\left(\frac{\partial E_z}{\partial y} - \frac{\partial E_y}{\partial z} + \sigma_x^e E\right) \\ \frac{\partial E_y}{\partial t} = \frac{1}{\varepsilon_y}\left(\frac{\partial H_x}{\partial z} - \frac{\partial H_z}{\partial x} - \sigma_y^e E_y\right), & \frac{\partial H_y}{\partial t} = -\frac{1}{\mu_y}\left(\frac{\partial E_x}{\partial z} - \frac{\partial E_z}{\partial x} + \sigma_y^e E\right) \\ \frac{\partial E_z}{\partial t} = \frac{1}{\varepsilon_z}\left(\frac{\partial H_y}{\partial x} - \frac{\partial H_x}{\partial y} - \sigma_z^e E_z\right), & \frac{\partial H_z}{\partial t} = -\frac{1}{\mu_z}\left(\frac{\partial E_y}{\partial x} - \frac{\partial E_x}{\partial y} + \sigma_z^e E\right) \end{cases} \tag{1}$$

Fig. 1 shows the simulation region of PhC UV LEDs in *x-y* plane and the cross-section in *y-z* plane. The PhC UV LEDs are fabricated by a hexagonal lattice array of AlGaN nanowires. In most situations in this paper, the height of nanowires is 1 μm, and the number of nanowires in each line is 11. The number of all the nanowires are 11 $\times$ 11. The radii and spacing of nanowires are normalized by the spacing and wavelength respectively for universal applications. To focus on the geometrical parameters of nanowires, the nanowire LEDs does not have other functional layers such as substrate, metal electrode, reflector, and so on. Each nanowire is comprised of a

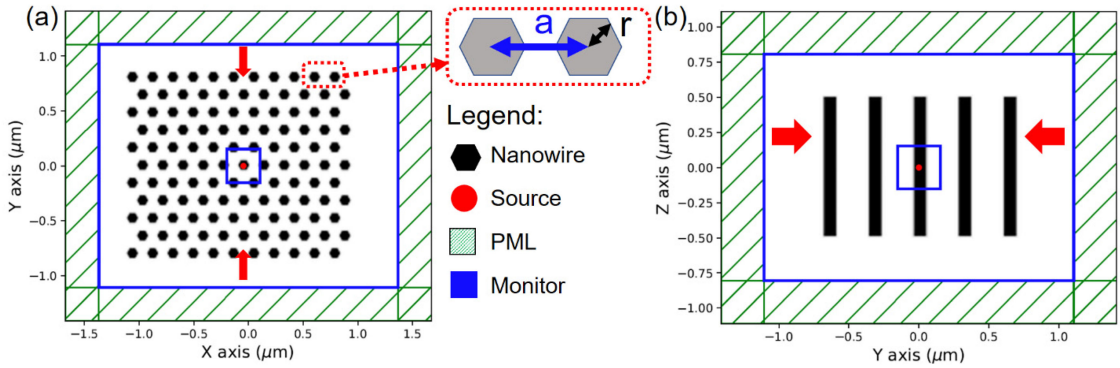

Fig. 1. The schematic diagram of FDTD simulation regions in the (a) *x-y* plane and (b) *y-z* plane. The red arrows point at the position of the cross-section in the *y-z* plane. a is the spacing of photonic crystal. *r* is the radius of the nanowire. The box monitors around the source are used to calculate the dipole source power. The large monitors next to the PML are used to calculate the LEE. Other detailed explanations for each part are in the legend.

unique material of AlGaN, which refractive index is 2.45 [4]. It is well-known that the active layers of LEDs consist of multiple AlGaN layers with different Al compositions. And these Al compositions correspond to the refractive index of these AlGaN layers. Thus, the impacts of refractive index of AlGaN layers will be discussed too. As shown in Fig. 1, a dipole source is located at the center of the device with TM polarization and random phase. The source spectrum is fitted with a Gaussian distribution, which center wavelength is 280 nm and the corresponding full width at half maximum (FWHM) is 10 nm. For a higher accuracy, there are 20 points per minimum wavelength in this discretized FDTD world. The monitors which are next to the perfectly matched layers (PML) are utilized to calculate the power propagating through a specific plane. The small box monitor around the dipole source is utilized to calculate the source power. To calculate the LEE defined as (2), all the powers through monitors are normalized by the source power. For example, the top LEE represents the normalized power propagating through the area of top monitor. And the side LEE is the sum of four lateral LEE around the device. The total LEE is the sum of top LEE and side LEE. The boundary layers around the simulation region are perfectly matched layers (PML) which are used to absorb outgoing waves. The region size is changed with the number of nanowires.

$$\text{LEE} = \frac{\text{Monitor power}}{\text{Source power}} \tag{2}$$

The band structure of PhC corresponding to the dispersion relation of AlGaN is calculated by MPB which is one of softwire packages in MEEP [14]. The equation on magnetic field $\mathbf{H}(\mathbf{r})$ in Maxwell equations can be combined in (3) which is treated as an eigenvalue problem. Thus, the magnetic field $\mathbf{H}(\mathbf{r}, t) = \mathbf{H}(\mathbf{r})e^{-i\omega t}$ is a harmonic mode as a mode profile times a complex exponential. Then, according to the electromagnetic variation theorem [15], the smallest eigenvalue ω^2/c^2 of (3) and its harmonic mode can be obtained by a minimization process. After the smallest eigenvalue, the following eigenvalues are obtained by iterating the minimization process until the photonic band structure of PhC are formed.

$$\nabla \times \left(\frac{1}{\varepsilon(r)} \nabla \times \mathbf{H}(\mathbf{r})\right) = \left(\frac{\omega}{c}\right)^2 \mathbf{H}(\mathbf{r}) \tag{3}$$

Due to a large index difference between the material and the surroundings, an AlGaN nanowire can be treated as an optical waveguide. According to the optical waveguide theory [16], the number of guided modes inside the nanowire can be obtained by solving their eigenvalue equations. Here, (4) is for HE_{vm} and EH_{vm} guided modes. Equation (5) is for TE_{0m} guided modes. And 6 is for TM_{0m} guided modes. HE_{vm}, EH_{vm}, TE_{0m}, TM_{0m} are different types of guided modes. n_1 and n_0

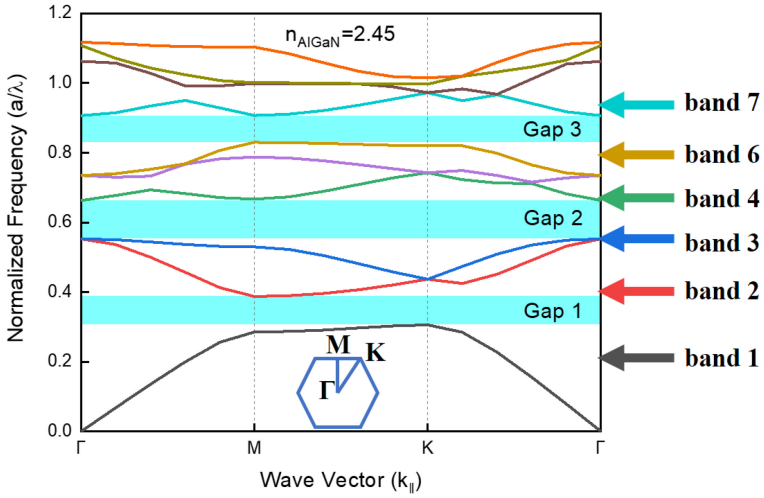

Fig. 2. The photonic band structure of the nanowire PhC for the in-plane propagation with TM polarization. The arrows point at the different photonic bands. There are three band gaps in the band structure. The special points at the center, face, and corner in the irreducible zone are known as Γ, *M*, and *K*.

are the refractive indexes of material and surroundings respectively. k is the wave vector. β_j is the propagation constant of the j^{th} guided mode. J_v is the Bessel function of the first kind, and K_v is the modified Bessel function of the second kind. U_j and W_j are dimensionless modal parameters defined by $U_j = r(k^2 n_1^2 - \beta_j^2)^{1/2}$ and $W_j = r(\beta_j^2 - k^2 n_0^2)^{1/2}$. V is the waveguide parameter defined by $V = 2\pi r/\lambda_0 \ (n_1^2 - n_0^2)^{1/2}$. r is the radius of nanowire. λ_0 is the light wavelength in the free-space. Exact solution for each guided mode can be found in our previous work [17].

$$\left\{\frac{J_v'(U)}{UJ_v(U)} + \frac{K_v'(W)}{WK_v(W)}\right\}\left\{\frac{J_v'(U)}{UJ_v(U)} + \frac{n_0^2 K_v'(W)}{n_1^2 WK_v(W)}\right\} = \left(\frac{v\beta_j}{kn_1}\right)^2\left(\frac{V}{UW}\right)^4 \tag{4}$$

$$\frac{J_1'(U)}{UJ_0(U)} + \frac{K_1'(W)}{WK_0(W)} = 0 \tag{5}$$

$$\frac{J_1'(U)}{UJ_0(U)} + \frac{n_0^2 K_1'(W)}{n_1^2 WK_0(W)} = 0 \tag{6}$$

3. Results and Discussion

Fig. 2 shows the photonic band structure of nanowire PhC. Here, a is the spacing of PhC, r is the radius of nanowire, λ is the wavelength of light. And $k_{\|}$ is the component of wave vector $\boldsymbol{k}$ in horizontal direction. Assume a normalized radius of a nanowire r/a is 0.35. It is shown in Fig. 2 that there are three photonic band gaps in the band structure. Gap 1 is located between Band 1 and Band 2. Gap 2 is located between Band 3 and Band 4. Gap 3 is located between Band 6 and Band 7. According to the properties of photonic band gap, when a normalized frequency is in a gap, the amplitude of light propagating inside the PhC would decay exponentially [15]. The frequency a/λ is normalized to the speed of light in a vacuum. It illustrates that these gaps can be used to suppress the propagation of light in the horizontal plane, and to couple the radiated modes with guided modes inside the nanowire, and finally to enhance the vertical LEE of UV LED [18]. However, do these three gaps have same efficiency for preventing the light horizontal propagation?

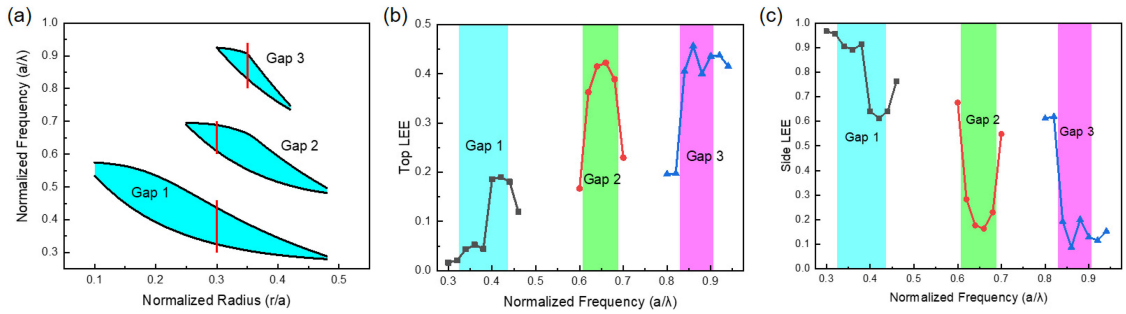

Fig. 3. (a) The gap map for TM polarization, the red lines correspond to the range in Fig. 3(b). (b) The top and (c) the side LEE ranges vary with the normalized frequencies which cross these three band gaps. The color bar represents the range of each band gap.

Fig. 3(a) shows a gap mapping corresponding to normalized frequency a/λ and normalized radius r/a. It is shown that all the edges of gaps decrease in normalized frequency a/λ as r/a increases. It can be explained that, since the normalized frequency scales as $1/\sqrt{\varepsilon}$ in a medium of dielectric constant ε , and as r/a increase, the average dielectric constant of material increases [15]. On the other hand, since the nanowires are contacted with each other as r/a is at 0.5, all the gaps become narrow and eventually disappear. By using the gap mapping, it is convenient to design the geometrical parameters of PhC. For example, assume the geometrical parameters of desired PhC in Gap 1. The wavelength of light is 280 nm. The normalized frequency and radius are chosen at 0.4 and 0.3 respectively. Then the spacing a is 112 nm calculated by 280×0.4. And the radius of nanowire is 33.6 nm calculated by 112×0.3. Subsequently, these calculated geometrical parameters of PhC can be checked by the FDTD method.

Fig. 3(b) and (c) show top and side LEE of PhC UV LEDs corresponding to three red lines crossing gaps in Fig. 3(a). These red lines are chosen randomly. The normalized radii r/a of red lines in Gap 1 and Gap 2 are 0.3, and it is 0.35 in Gap 3. There are three phenomena needed to be discussed. Firstly, Fig. 3(c) shows that all the side LEE outside gaps are much higher than them inside the gaps. It means all the gaps have an ability to prevent the horizontal propagation of light. At the same time, the corresponding top LEE in gaps are higher than them outside the gap. It means that those inhibiting light in horizontal direction are coupled with the modes in vertical direction by gaps. Secondly, the side LEE of both Gap 2 and Gap 3 are much lower than them in Gap 1. As a contrast, the top LEE of both Gap 2 and Gap 3 are much higher than them in Gap 1. It illustrates that the inhibiting ability of Gap 1 is weaker than Gap 2 and Gap 3. Thirdly, the top LEE does not increase or the side LEE does not decrease as a/λ increases in each gap, but the highest top LEE or the lowest side LEE is at the center of each gap. Thus, it is necessary to have a detailed study as follow.

Fig. 4(b)–(d) show the field profiles of three devices which geometrical parameters correspond to the highest top LEE in each gap in Fig. 3(b). The normalized frequencies a/λ are at 0.4, 0.66 and 0.86 respectively in Fig. 4(b), (c), and (d). The wavelength λ is 280 nm. Then, the radii of nanowires are 33.6, 55.44 and 84.28 nm respectively calculated by $r/a \times a/\lambda \times \lambda$. It is observed in field profiles that, as the radii of nanowires grow, the radiated modes in horizontal direction decrease, and the guided modes along the axis of nanowire increase. It can be explained by the optical waveguide theory [16], [19]. The number of guided modes are calculated by solving their eigenvalue equations. Fig. 4(a) shows that the number of guided modes increases with the growth of radius. Thus, a nanowire with bigger radius supports more guided modes to couple with radiated modes. So, the devices which parameters in Gap 2 and Gap 3 have more light escaped from the top face. As a comparison, the devices which parameters in Gap 1 cannot support enough guided modes to couple with those radiated modes. So, the top LEE in Gap 1 are much lower than them in Gap 2 and Gap 3. And the side LEE in Gap 1 are much higher than them in Gap 2 and Gap 3.

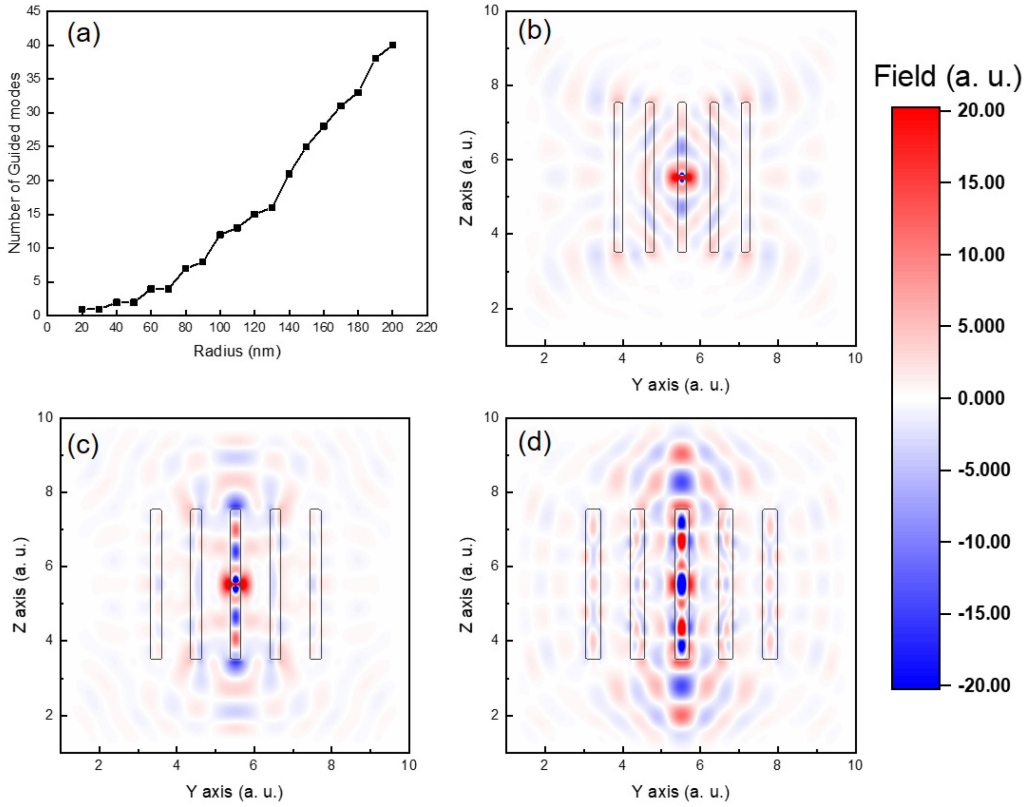

Fig. 4. (a) The number of guided modes increases with the growth of radius. The field profiles of three devices in the y-z plane correspond to the highest top LEE in each gap in Fig. 3(b). The corresponding normalized frequencies a/λ are (b) 0.4, (c) 0.66 and (d) 0.86, respectively.

However, it seems that the variation of LEE inside each gap does not obey the optical waveguide theory. As the radius grows, there is a peak top LEE or a valley side LEE inside every gap. This phenomenon can be explained by the variation of field profiles. Fig. 5 shows the variations of field profiles corresponding to the red line on Gap 2 in Fig. 3(a). It has been mentioned that Gap 2 locates between the Band 3 and Band 4. Since the red line on Gap 2 is larger than the range of corresponding gap, Fig. 5(a) and (b) show the field distribution in Band 3 and Band 4 respectively. It can be observed that, as a/λ increases, the intensity of guided modes inside nanowire becomes stronger gradually. Particularly the radiated modes nearly disappear when a/λ is at 0.66. With the continuous growth of a/λ, the radiated modes become stronger and the guided modes become weaker. It illustrates that, although the radiated modes are inhibited by the optical gaps, they are still affected by the optical bands next to the gaps. The center position of a gap, which is far away both two side bands, corresponds to the strongest inhibiting ability. This phenomenon can also be observed in the far-field distribution obviously as shown in Fig. 6. When a/λ is at 0.66, those radiated modes in horizontal direction almost disappear. As a contrast, the intensity in vertical direction are relatively strong. However, no matter a/λ increases or decreases from the center of a gap, the radiated modes in horizontal direction appear gradually. Thus, when the normalized frequency a/λ of light locates in the middle of a gap, the guided modes inside the nanowire have the highest coupling efficiency.

For a fair comparison, Fig. 7 shows LEE mappings in all gaps corresponding to gap mappings in Fig. 3(a). The range and step of data is shown in Table 1. It is shown that most top LEE in Gap 2 and Gap 3 are higher than them in Gap 1. At the same time, most side LEE in Gap 2 and

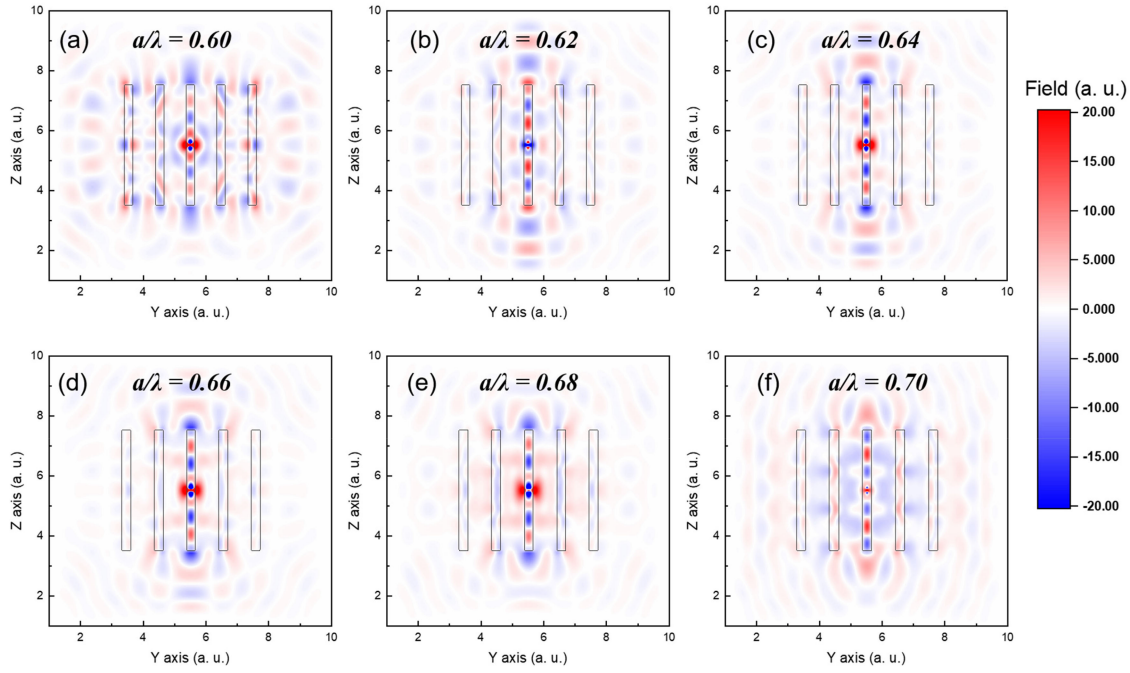

Fig. 5. The field profile of PhC in the *y-z* plane with the variation of normalized frequency a/λ. The various normalized frequencies are (a) 0.60, (b) 0.62, (c) 0.64 (d) 0.66, (e) 0.68, (f) 0.70. The range of the normalized frequency covers Gap 2. The normalized radius is 0.3. The wavelength is 280 nm.

TABLE 1
The Range of the Values for LEE Mappings in Fig. 7

	r/a	band edge of a/λ	Chosen ranges of a/λ	step of a/λ
Gap 1	0.1	0.5336-0.5747	0.52-0.58	0.02
	0.2	0.3924-0.5351	0.38-0.54	0.02
	0.3	0.3253-0.4363	0.30-0.46	0.02
	0.4	0.2926-0.3449	0.28-0.36	0.02
Gap 2	0.3	0.6089-0.6893	0.60-0.70	0.02
	0.35	0.5529-0.6632	0.54-0.68	0.02
	0.4	0.5149-0.5935	0.50-0.60	0.02
Gap 3	0.32	0.8833-0.9216	0.86-0.94	0.02
	0.35	0.8297-0.9067	0.80-0.94	0.02
	0.38	0.7846-0.8351	0.76-0.86	0.02

Gap 3 are lower than in Gap 1. It illustrates that a major portion of geometrical parameters in both Gap 2 and Gap 3 is more suitable to enhance vertical LEE than them in Gap 1. However, as shown in Fig. 7(d), most total LEE in Gap 1 are near the unit and much higher than them in Gap 2 and Gap 3. Considering the concept of total LEE in this paper, it can be explained that the rest of light in Gap 2 and Gap 3 propagates toward the substrate of devices as down LEE shown in Fig. 7(c). Thus, to modify top LEE in Gap 2 and Gap 3, some reflective layers on substrates are necessary [20].

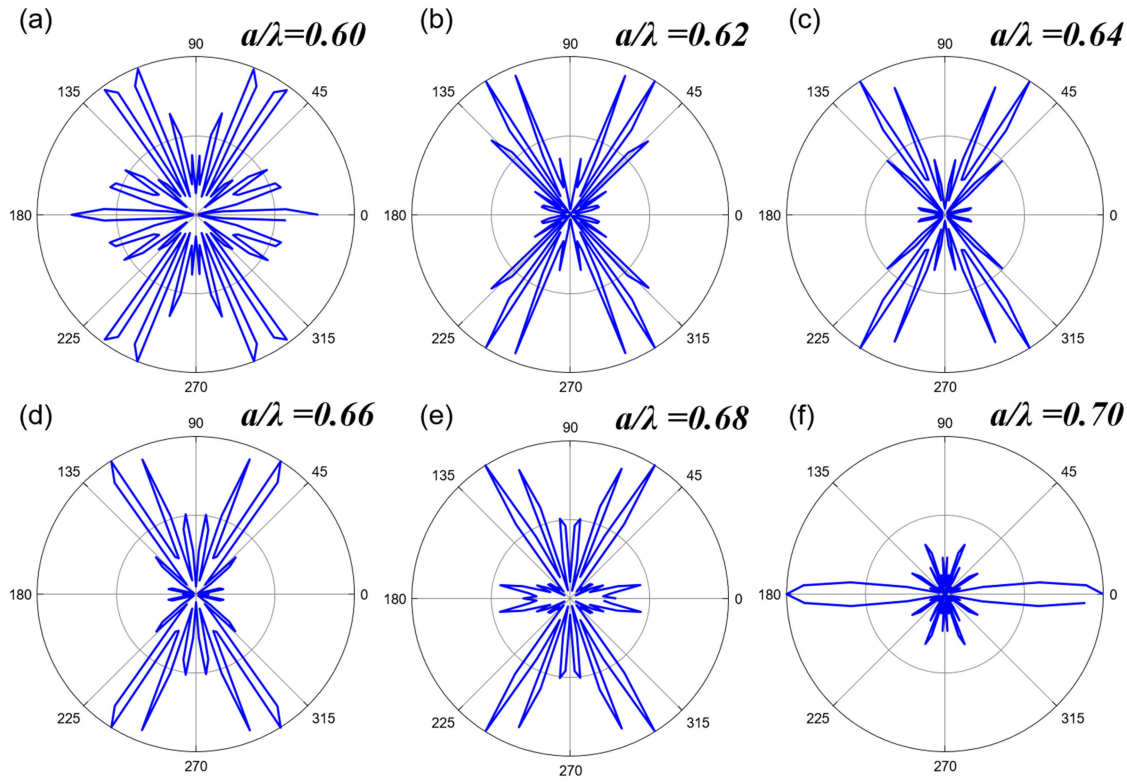

Fig. 6. The far-field distributions of PhC in the *y-z* plane with the variation of normalized frequency a/λ. The geometrical parameters are the same with them in Fig. 5. The various normalized frequencies are (a) 0.60, (b) 0.62, (c) 0.64 (d) 0.66, (e) 0.68, (f) 0.70. The range of the normalized frequency covers Gap 2. The normalized radius is 0.3. The wavelength is 280 nm.

The impacts of nanowire height on LEE are discussed. Fig. 8(a) shows that top LEE have a fluctuating increase, and the side LEE decease at the same time. It can be explained by the mode profiles in Fig. 8(b)-(c). Due to total internal reflection (TIR) at the AlGaN/air interface, a nanowire can be treated as a Fabry-Perot resonant cavity. Fig. 8(c) shows that, when the height of nanowire is at 1.4 μm, the intensity inside the nanowire is weakened by the resonance. As a contrast, when the height is at 1.5 μm, the intensity obviously strengthen. The resonance is related to the propagation phases of guided modes. The phase difference between mode phases is affected by the light path. The light path is decided by the length of the cavity [21]. Thus, the growth of cavity length makes the intensity of the resonance changed periodically. On the other hand, the growth of height increases the lateral surface area of nanowire. As a result, it increases few lateral emission of light. Thus, as height grows, the side LEE has an increasing trend, and the top LEE decrease slowly.

The impacts of number of nanowires are discussed. Fig. 9(a) and (b) show the variation of top and side LEE related to the number of nanowires in each line in PhC. As the number of nanowires increases, the side LEE decrease slowly, and the top LEE increase at the same time. It is easily understood that an addition of the number nanowires increases the scattering of light in horizontal direction. For a practical comparison, there is a dipole source at the center of each nanowire. It means that, the number of dipole sources equals to the number of nanowires. The results of multiple dipole sources simulations are shown in Fig. 9(a)-(b). The top LEE with multiple dipole sources are lower than them with a single dipole source. At the same time, the side LEE with multiple dipole sources are higher than them with a single dipole source. The reason is that, the radiated modes emitted from the nanowires near the edges of device cannot be efficiently inhibited

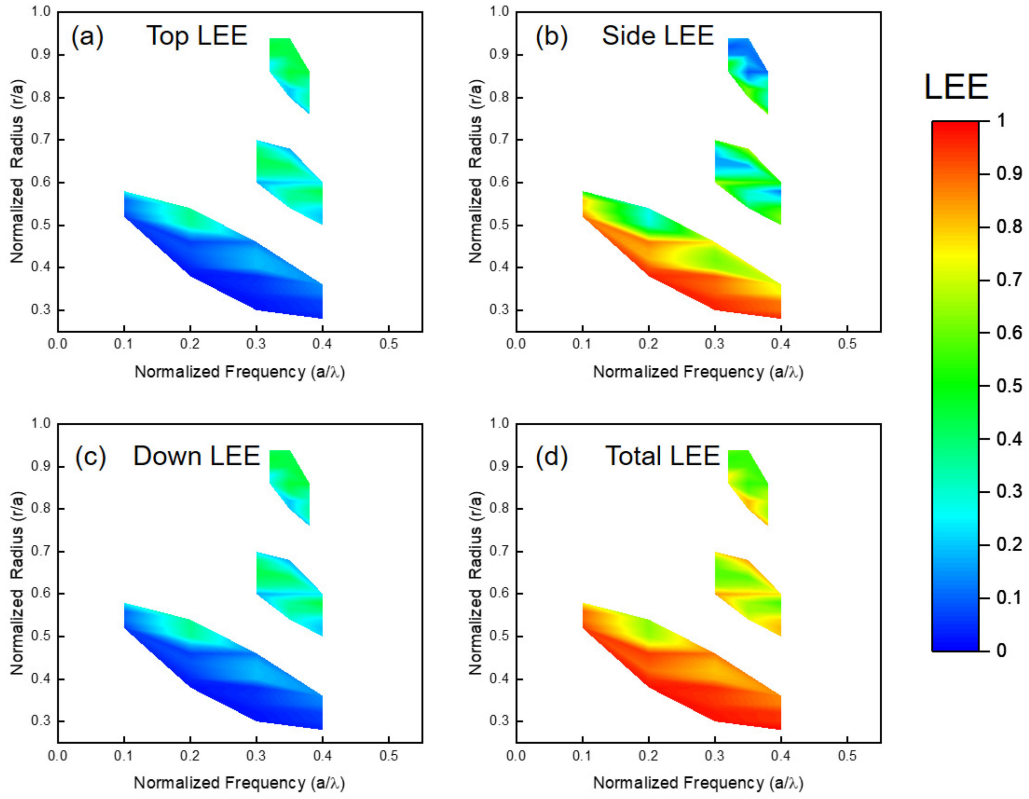

Fig. 7. The mappings of (a) top LEE, (b) side LEE, (c) down LEE and (d) total LEE.

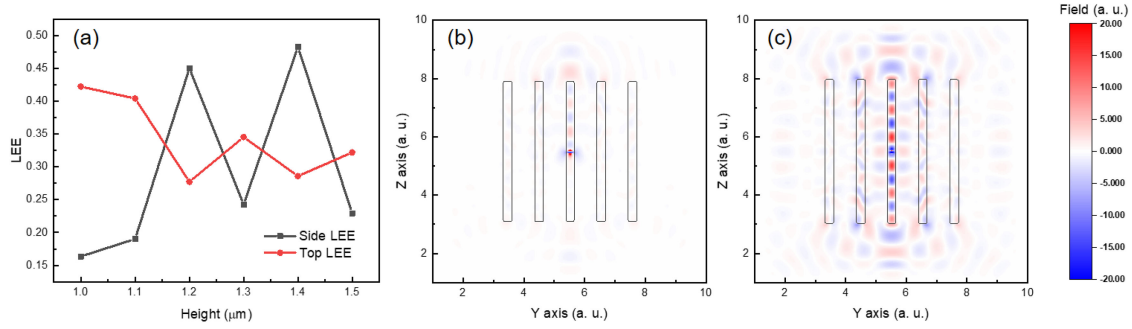

Fig. 8. (a) The top and the side LEE changes with the growth of the height of nanowire. The field profiles in the *y-z* plane are at the heights of (b) 1.4 μm and (c) 1.5 μm. The normalized frequency a/λ of 0.66 and the normalized radius of 0.3 corresponds to the lowest side LEE in Gap 2, as shown in Fig. 3(b).

by the photonic band gap. Consequently, there are always some radiated modes escaping from the lateral side of device. The side LEE with multiple dipole sources are obviously higher than them with single dipole source. Fortunately, as the number of nanowires increases, the side LEE with multiple dipole sources decrease, and the top LEE enhances, which is similar with them with a single dipole source. The reason is that the extra additional lights are more than the escaped lights from the nanowires at the edge of devices on the whole. So the increase of number can efficiently weaken the surface effects on LEE.

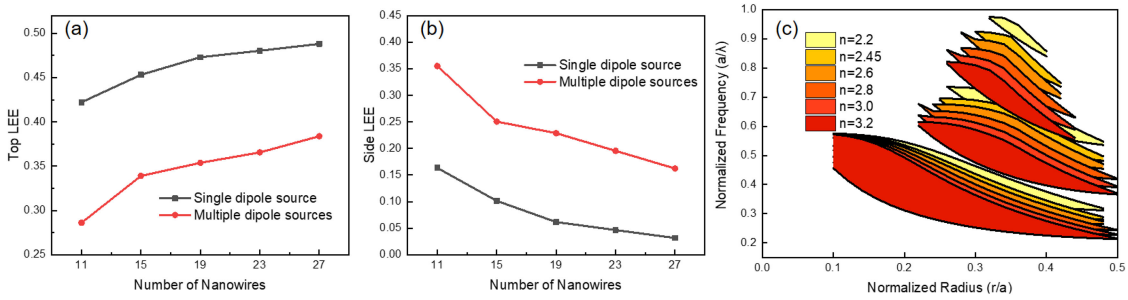

Fig. 9. (a) The top LEE and (b) the side LEE change with the growth of the number of nanowires. The single dipole source means there is one dipole source inside the device. The multiple dipole sources mean there is a dipole source inside each nanowire. The nanowire number here is the number of nanowires in each line. The normalized frequency, the normalized radius, and the wavelength are 0.66, 0.3, and 280 nm, respectively. (c) The optical band gap mapping changes with an increase of refractive indexes of AlGaN layers.

The impacts of refractive index are discussed. It is known that an ultraviolet LEDs contain multiple AlGaN-based layers with various Al compositions. The changed Al compositions of AlGaN layers lead to a variation of refractive index. Fig. 9(c) shows the band gap mappings changed with an increase of refractive indexes of AlGaN layers. The range of refractive indexes are chosen from 2.2 to 3.2 [22], [23]. It illustrates that, assuming the wavelength of light and the spacing of PhC are fixed, the radii of nanowires decrease as the refractive index increases corresponding to a same point in a gap. It can be explained by the concept of waveguide parameter $V = 2\pi r/\lambda_0(n_1^2 - n_0^2)^{1/2}$. A higher refractive index of material n_1 increases the corresponding waveguide parameter. And both the waveguide parameter V and nanowire radius r are in proportion to the number of guided modes. Thus, the increase of refractive index leads to a decrease of the waveguide parameter, and then the nanowire radius. As a whole, all the gaps move toward down in gap mappings. On the other hand, considering the difference of refractive indexes of AlGaN multiple layers, the gap overlap at different indexes may be a better choice to enhance the top LEE. This situation will be study in the future.

4. Conclusion

All the photonic band gaps of nanowire PhC can inhibit the horizontal propagation of light and enhance the vertical LEE of UV LEDs. However, the inhibiting ability of Gap 1 is obviously weaker than them of both Gap 2 and Gap 3. The reason is that the radii of nanowires in Gap 1 are too small. As a result, there are not enough guided modes inside the nanowires to couple with the radiated modes. Thus, the nanowires in Gap 2 and Gap 3 are more suitable to design a PhC structure of UV LEDs. Nevertheless, a reflected layer between the nanowires and substrate are still necessary to prevent the absorption of substrate. In addition, as a growth of nanowire height, the top LEE fluctuates widely due to the resonance, and decreases gradually due to the increase of lateral surface area. The top LEE also enhances with the increase of the number of nanowires since the extra additional lights are more than the escaped lights from the nanowires at the edge of devices on the whole. Thus, more nanowires inside PhC UV LEDs have benefits to achieve a higher vertical LEE. This work can be treated as guidelines for the practical production of nanowire PhC UV LEDs.

References

[1] N. Gao, K. Huang, J. Li, S. Li, X. Yang, and J. Kang, "Surface-plasmon-enhanced deep-UV light emitting diodes based on AlGaN multi-quantum wells," *Sci. Rep.*, vol. 2, no. 1, pp. 816–816, 2012.

[2] H. Chen, H. Fu, Z. Lu, X. Huang, and Y. Zhao, "Optical properties of highly polarized InGaN light-emitting diodes modified by plasmonic metallic grating," *Opt. Exp.*, vol. 24, no. 10, pp. A856–A867, 2016.
[3] S. Wang *et al.*, "Ultrahigh degree of optical polarization above 80% in AlGaN-based deep-ultraviolet LED with moth-eye microstructure," *ACS Photon.*, vol. 5, no. 9, pp. 3534–3540, Sep. 2018.
[4] M. Djavid and Z. Mi, "Enhancing the light extraction efficiency of AlGaN deep ultraviolet light emitting diodes by using nanowire structures," *Appl. Phys. Lett.*, vol. 108, no. 5, 2016, Art. no. 051102.
[5] S. Zhao, R. Wang, S. Chu, and Z. Mi, "Molecular beam epitaxy of iii-nitride nanowires: Emerging applications from deep-ultraviolet light emitters and micro-LEDs to artificial photosynthesis," *IEEE Nanotechnol. Mag.*, vol. 13, no. 2, pp. 6–16, Apr. 2019.
[6] P. Du, Y. Zhang, L. Rao, Y. Liu, and Z. Cheng, "Enhancing the light extraction efficiency of AlGaN LED with nanowire photonic crystal and graphene transparent electrode," *Superlattices Microstruct.* vol. 133, p. 106216, 2019.
[7] X. H. Liu, K. Mashooq, T. Szkopek, and Z. T. Mi, "Improving the efficiency of transverse magnetic polarized emission from AlGaN based LEDs by using nanowire photonic crystal," *IEEE Photon. J.,* vol. 10, no. 4, Aug. 2018, Art. no. 4501211.
[8] P. Du and Z. Cheng, "Enhancing light extraction efficiency of vertical emission of AlGaN nanowire light emitting diodes with photonic crystal," *IEEE Photon. J.*, vol. 11, no. 3, Jun. 2019, Art. no. 1600109.
[9] M. Djavid *et al.*, "Effects of optical absorption in deep ultraviolet nanowire light-emitting diodes," *Photon. Nanostruct.*, vol. 28, pp. 106–110, Feb. 2018.
[10] R. Lin *et al.*, "Tapering-induced enhancement of light extraction efficiency of nanowire deep ultraviolet LED by theoretical simulations," *Photon. Res.,* vol. 6, no. 5, pp. 457–462, 2018.
[11] A. F. Oskooi, D. Roundy, M. Ibanescu, P. Bermel, J. D. Joannopoulos, and S. G. Johnson, "MEEP: A flexible free-software package for electromagnetic simulations by the FDTD method," *Comput. Phys. Commun.*, vol. 181, no. 3, pp. 687–702, Mar, 2010.
[12] J. B. Schneider, "Understanding the finite-difference time-domain method," 2010. [Online]. Available: http://www.eecs.wsu.edu/∼schneidj/ufdtd, 2017
[13] A. Elsherbeni and V. Demir, *The Finite-Difference Time-Domain Method for Electromagnetics with MATLAB Simulations*, Raleigh, NC, USA: SciTech Publishing, Inc., 2006.
[14] S. G. Johnson and J. D. Joannopoulos, "Block-iterative frequency-domain methods for maxwell's equations in a planewave basis," *Opt. Exp.*, vol. 8, pp. 173–190, 2001.
[15] J. D. Joannopoulos *et al.*, *Photonic Crystals: Molding the Flow of Light*. Princeton, NJ, USA: Princeton Univ. Press, 2007.
[16] A. W. Snyder and J. D. Love, *Optical Waveguide Theory*. London, U. K.: Chapman and Hall, 1983.
[17] Z. Zhang, F. Gao, and G. Li, "The impact of resonance on the light extraction efficiency of single nanowire ultraviolet light emitting diodes," *IEEE Photon. J.*, vol. 12, no. 4, Aug. 2020, Art. no. 8200610.
[18] A. David, H. Benisty, and C. Weisbuch, "Photonic crystal light-emitting sources," *Rep. Prog. Phys.*, vol. 75, no. 12, Dec. 2012, Art. no. 126501.
[19] L. Tong, J. Lou, and E. Mazur, "Single-mode guiding properties of subwavelength-diameter silica and silicon wire waveguides," *Opt. Exp.*, vol. 12, no. 6, pp. 1025–1035, 2004.
[20] Y. Wu, Y. Wang, K. Sun, and Z. Mi, "Molecular beam epitaxy and characterization of AlGaN nanowire ultraviolet light emitting diodes on al coated si (0 0 1) substrate," *J. Cryst. Growth*, vol. 507, pp. 65–69, 2019.
[21] I. Friedler, C. Sauvan, J. P. Hugonin, P. Lalanne, J. Claudon, and J. M. Gérard, "Solid-state single photon sources: The nanowire antenna," *Opt. Exp.*, vol. 17, no. 4, pp. 2095–2110, 2009.
[22] K. Takeuchi, S. Adachi, and K. Ohtsuka, "Optical properties of $al_xGa_{1-x}N$ alloy," *J. Appl. Phys.*, vol. 107, no. 2, 2010, Art. no. 023306.
[23] N. A. Sanford *et al.*, "Refractive index study of $Al_xGa_{1-x}N$ films grown on sapphire substrates," *J. Appl. Phys.*, vol. 94, no. 5, pp. 2980–2991, 2003.